


RESEARCH ARTICLE

Surface moisture area during rainfall–run-off events to understand the hydrological dynamics of a basin in a plain region

María Guadalupe Ares^{1,2,3}  | Mauro Holzman^{1,2} | Ilda Entraigas^{2,4,5} | Marcelo Varni² | Luisa Fajardo^{2,3,4} | Natalia Vercelli^{1,2,5}

¹ Consejo Nacional de Investigaciones Científicas y Técnicas, 1917 Rivadavia Avenue, Buenos Aires C1033AAJ, Argentina

² Instituto de Hidrología de Llanuras 'Dr EJ Usunoff', 780 República de Italia Avenue, Azul 7300Buenos Aires Province, Argentina

³ Facultad de Ingeniería, Universidad Nacional del Centro de la Provincia de Buenos Aires, 5737 Del Valle Avenue, Olavarría 7400Buenos Aires province, Argentina

⁴ Comisión de Investigaciones Científicas de la Provincia de Buenos Aires, 526 street between 10 and 11 streets, La Plata 1900Buenos Aires Province, Argentina

⁵ Facultad de Agronomía, Universidad Nacional del Centro de la Provincia de Buenos Aires, 780 República de Italia Avenue, Azul 7300Buenos Aires Province, Argentina

Correspondence

María Guadalupe Ares, Consejo Nacional de Investigaciones Científicas y Técnicas, 1917 Rivadavia Avenue, Buenos Aires C1033AAJ, Argentina.

Email: gares@faa.unicen.edu.ar

Abstract

The understanding of the hydrology of plain basins may be improved by the combined analysis of rainfall–run-off records and remote sensed surface moisture data. Our work evaluates the surface moisture area (SMA) produced during rainfall–run-off events in a plain watershed of the Argentine Pampas Region, and studies which hydrological variables are related to the generated SMA. The study area is located in the upper and middle basins of the Del Azul stream, characterized by the presence of small gently hilly areas surrounded by flat landscapes. Data from 9 rainfall–run-off events were analysed. MODIS surface reflectance data were processed to calculate SMA subsequent to the peak discharge (post-SMA), and previous to the rainfall events (prev-SMA), to consider the antecedent wetness. Rainfall–run-off data included total precipitation depth (P), maximum intensity of rainfall over 6 hr (I_{6max}), surface runoff registered between the beginning of the event and the day previous to the analysed MODIS scene (R), peak flow (Q_p), and flood intensity (IF). In contrast with other works, post-SMA showed a negative relationship with the R. Three groups of cases were identified: (a) Events of low I_{6max} , high prev-SMA, and low R were associated with slow and weakly channelized flow over plain areas, leading to saturated overland flow (SOF), with large SMA; (b) events of high I_{6max} , low prev-SMA, and medium to high R were rapidly transported along the gentle slopes of the basin, related to Hortonian overland flow (HOF) and low post-SMA; and (c) events of medium to high I_{6max} and prev-SMA with medium R were related to heterogeneous *input-antecedent-run-off* conditions combined: Local spatial conditions may have produced HOF or SOF, leading to an averaged response with medium SMA. The interactions between the geomorphology of the basin, the characteristics of the events, and the antecedent conditions may explain the obtained results. This analysis is relevant for the general knowledge of the hydrology of large plains, whose functioning studies are still in their early stages.

KEYWORDS

gentle hills and slopes, hydrological variables, plain areas, rainfall–run-off events, run-off generation mechanisms, surface moisture area

1 | INTRODUCTION

The analysis of surface water dynamics is essential to understand the processes involved in the hydrological response of watersheds. Those processes are the result of complex interactions between land use, soil properties, antecedent conditions, and rainfall characteristics (Rodríguez-Blanco, Taboada-Castro, & Taboada-Castro, 2012). Hortonian overland flow, saturation overland flow, and throughflow are recognized as the mechanisms by which rainwater reaches streams (Dingman, 2015). Topography is a key controlling factor of these hydrological mechanisms: It is involved in the development of soil and, as a consequence, in its vegetation cover, which are closely related to surface run-off potential (Dunne, Moore, & Taylor, 1975; Mc Donnell, 2013; Smith & Goodrich, 2005).

Hydrology of large plains differs considerably from that of hilly and mountainous areas. Although the components of the hydrological cycle are the same in both areas, their interaction and relative importance are different (Paoli & Giacosa, 1983). Extensive plains are characterized by the presence of shallow local depressions instead of a clearly developed river network (Dalponte et al., 2007). When these areas are affected by floods, water is accumulated in such depressions and moves very slowly as sheet flow. This is a consequence of the low morphological energy-content of this hydrological system, due to the low regional slopes, and the vertical movement of water dominates over its horizontal movement (Kovács, 1983; Kruse & Zimmermann, 2002). Thus, infiltration and evapotranspiration are the main mechanisms by which most of the water discharges (Varni, Usunoff, Weinzettel, & Rivas, 1999).

Argentine Pampas Region is a plain of over 1.5 million km², with lands of high fertility and productivity (Quiroz Londoño, Romanelli, Lima, Massone, & Martínez, 2016). There, 90% of the country's grain production takes place (Magrin, Travasso, & Rodríguez, 2005), and 48% of the cattle stock is raised (Canosa, Feldkamp, Urruti, Morris, & Moscoso, 2013), because it is the most productive rain-fed and the strongest economic region of Argentina (Holzman, Rivas, & Bayala, 2014). In this region, there are gently hilly areas which occupy a small portion with respect to that occupied by plains: only 13% of the region (Mateucci, 2012). Thus, these areas are of local importance on hydrology, with well drained and sloped landscapes where water outflows horizontally in a river network. Run-off from these areas reaches the neighbouring plains and vanishes or moves over the surface and contributes to increase water storage, evapotranspiration, or water outflows by connections between overflowing depressions (Aragón, Jobbágy, & Viglizzo, 2010; Dalponte et al., 2007). The Pampas Region is periodically affected by large floods. When flooded, some depressions discontinue their agricultural production and temporarily become sites for wildlife. Thus, the study of the dynamics of areas under humid conditions is of special interest for land use decision makers from different points of view.

The joint analysis of different hydrological variables improves the understanding of the hydrological functioning of an area (Latron & Gallart, 2008; Wu & Liu, 2015). The application of satellite imagery for detecting surface water has been widely used worldwide with different purposes: floodplain and wetland inundation mapping (Chen, Huang, Ticehurst, Merrin, & Thew, 2013; Huang, Chen, & Wu, 2014;

Klein et al., 2014), hydrologic model calibration (Khan et al., 2011), or to detect the changes in water bodies areas (Baker, Lawrence, Montagne, & Patten, 2007; Rokni, Ahmad, Selamat, & Hazini, 2014; Varni, Entraigas, Migueltorena, & Comas, 2013). However, the relationships between remote sensed data for run-off events and the corresponding hydro climatic registered variables have not been frequently analysed. In this sense, Frazier, Page, Louis, Briggs, and Robertson (2003) related wetland inundation to river discharge, whereas Hamilton, Sippel, and Melack (2002) and Papa, Prigent, and Rossow (2008) related the monthly flooded area to river stage in large plain basins.

The objectives of this work are to assess the surface moisture area (SMA) generated during rainfall-run-off events and to analyse which hydrological variables are related to the moisture area in a plain basin of the Pampas Region. In addition, this manuscript discusses the dynamics of possible hydrological processes in the basin. At a regional scale, the study area is representative of other non-typical hydrological systems associated with plain areas of the world. At a local scale, the basin is characterized by the coexistence of a small gently hilly area with a neighbouring flat landscape which causes a particular hydrological behaviour. The hydrological dynamics at this and other comparable plain areas around the world (e.g., Brazilian Pantanal, Orinoco Llanos in Colombia and Venezuela, the plains of Manitoba and Saskatchewan in Canada, the plains at the east of Europe and Western Siberia, and those located at the east of Australia, among others) is complex and needs further research and investigation because its understanding is still not complete (Aragón et al., 2010; Dalponte et al., 2007; Jobbágy, Noretto, Santoni, & Baldi, 2008; Scioli, 2016; Viglizzo et al., 2009). This manuscript discusses the relationships between remote sensed SMA, and a set of hydrological variables registered or calculated during rainfall-run-off events in the watershed, on a daily basis. The results of this novel analysis for the Pampas Region are considered key for the adjustment of prediction models implemented by decision makers.

2 | MATERIALS AND METHODS

2.1 | Study area

Del Azul basin is located in the Argentine Pampas Region, between 36°00' and 37°20' S and between 60°15' and 58°45' W. The climate is temperate humid with an average annual temperature of 14.4°C. The average annual rainfall is 912 mm and 71% occurs between October and April.

The study was carried out in the area covered by the upper and middle basins of the Del Azul stream (Figure 1), which has an area of 981 km². According to the geomorphology described by Zárate and Mehl (2010) and to the topography analysed by Sala, Kruse, and Aguglino (1987), the upper sector of the watershed is located in the *Dominio Serrano (Range Domain)*, and the middle sector in the *Dominio Extraserrano (Extra-range Domain)* of the Del Azul basin. The upper sector is characterized by watershed divides and valleys. Watershed divides include two geomorphological units: summits and plain areas. Summits are between 280 and 400 masl, with slopes which exceed 5%. The plain areas, with average slopes of 0.9%, constitute the

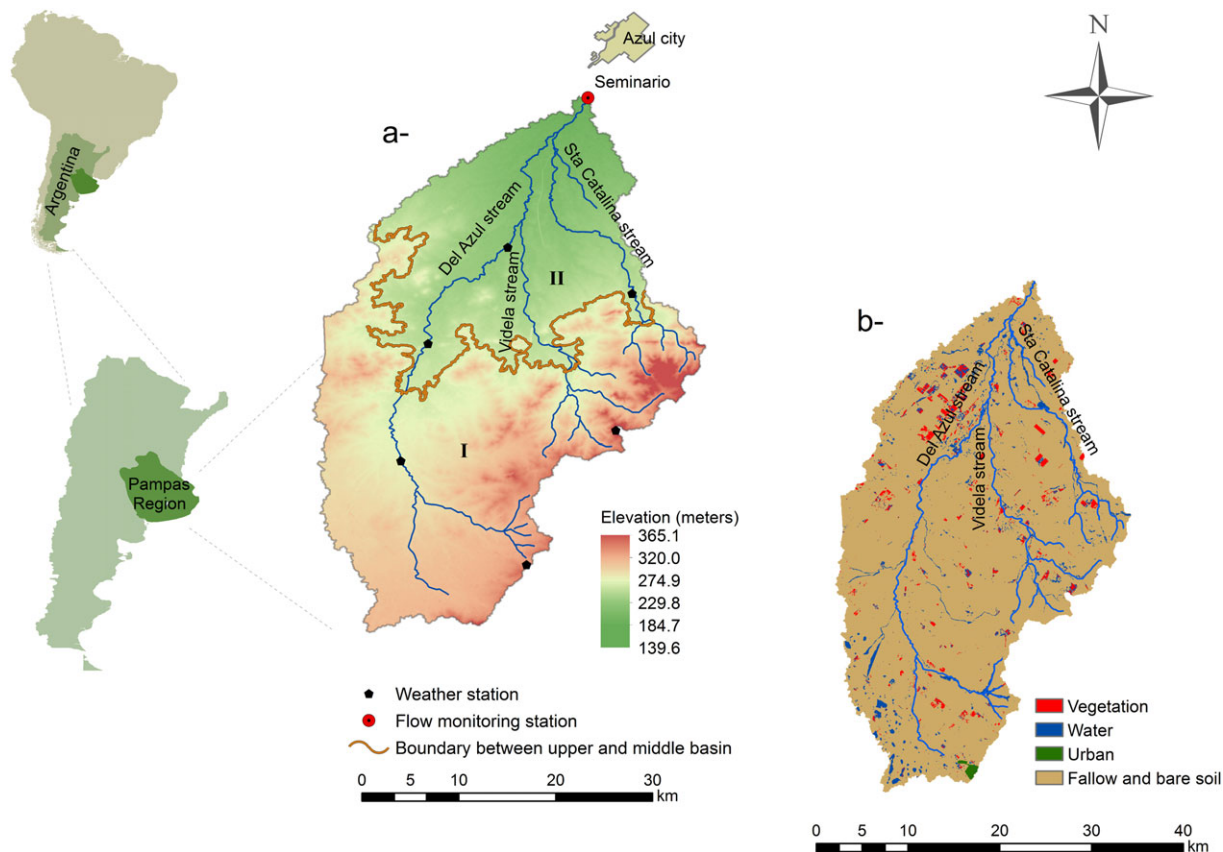


FIGURE 1 (a) Location of the upper (I) and middle (II) basin of the Del Azul. Weather stations and flow monitoring station (Seminario), (b) land use corresponding to winter 2013

headwaters of the drainage network, where, in addition, some wetlands are located. A shallow loess-like deposit (<1 m) above a calcareous crust—a layer formed by silts cemented by calcium carbonate locally known as *tosca* (INTA (Instituto Nacional de Tecnología Agropecuaria), 1989)—covers the plain areas. Valleys occupy the area between the hillsides and the flood plains, where isolated mounds with gentle slopes constitute secondary watershed divides with a moderately undulating relief. Floodplains are narrow strips along the water courses, with low relief and poor drainage.

The middle basin is located between the foot of slopes of rock outcrops and Azul city, which is situated at 130 masl. It is a plain with gentle hills and slopes ranging from 0.2% to 2%, covered by aeolian sediments with a thickness between 0.8 and 1 m above a calcareous crust.

Considering the soil cartography of Argentina published by INTA (Instituto Nacional de Tecnología Agropecuaria; 1992), Argiudolls and Hapludolls are the predominant soil classes in the study watershed. These soils may be shallow in the hilly areas by the presence of rock or by the calcareous crust previously mentioned. Natraqualfs and Natracuolls occupy the adjacent area to the water courses. Agriculture and cattle fattening are the main land uses in the study area. Rotations include mainly winter crops (wheat and barley), summer crops (soybean, corn, or sunflower), and pastures in less proportion.

2.2 | Surface moisture area

Moderate Resolution Imaging Spectroradiometer (MODIS)-based products were analysed and processed to calculate SMA subsequent

to the peak discharge and previous to the rainfalls which caused the run-off events, to consider the antecedent wetness. The products were acquired from the National Aeronautics and Space Administration's Earth Observing System Data and Information System (<http://reverb.echo.nasa.gov/reverb>). Those included scenes of the product MYD09GQ version 5: daily MODIS/Aqua surface reflectance at 250-m resolution (provides estimates of the surface spectral reflectance corrected of atmospheric scattering and absorption), level 2G. This product includes surface reflectance for Band 2 (near-infrared or NIR, 841–876 nm bandwidth) and Band 1 (Red, 620–670 nm bandwidth). This medium spatial resolution is appropriate for analyses at regional and local scales (Hansen, Townshend, DeFries, & Carroll, 2005; Holzman & Rivas, 2016; Holzman, Rivas, & Piccolo, 2014). In addition, the daily temporal resolution of this product increases the chances of finding cloud-free images coinciding with the rainfall-run-off events.

The main advantages of reflectance-based methods estimating SMA are (a) mature technology and (b) high spatial resolution in comparison to other types of sensor (e.g., microwave instruments). However, the main disadvantages are (a) no data availability under cloudy sky and (b) limited ability to penetrate vegetation canopy and soil (Petropoulos, Ireland, & Barrett, 2015). On the other hand, microwave methods are robust techniques to estimate surface soil moisture. However, the main limitation is the coarse spatial or temporal resolution. Also, there are other issues as surface roughness effect, low penetration depth in saturated, or near-saturated soils (Li, Crow, & Kustas, 2010; Njoku & Entekhabi, 1996).

The relationship between reflectance in different bands of the electromagnetic radiation spectrum and surface soil moisture has been studied extensively (e.g., Gao et al., 2013; Lobell & Asner, 2002). Several studies have demonstrated that reflectance in the solar spectrum domain decreases with soil moisture increase, and this property has been used to estimate soil moisture (Ahmad, Zhang, & Nichols, 2011; Ghulam, Qin, Teyip, & Li, 2007; Jensen, 2007; Milfred & Kiefer, 1976; Weidong et al., 2002).

Also, diverse works show that the longer the wavelength in the optical domain (400–2,500 nm), the better potential to detect soil moisture (e.g., Sriwongsitanon et al., 2015; Zhu et al., 2010). Thus, Band 2 (NIR) is an appropriate alternative to identify not only moist soil but also flooded areas (Amani, Parsian, Mirmazloui, & Aieneh, 2016; Brakenridge & Anderson, 2006; Gao et al., 2013). It is important to note that the surface horizons of dominant soils in the study area are well-structured clay loam and silty clay loam soils. Thus, near surface soil moisture has influence on surface soil moisture, associated with capillary action, and so, in surface reflectance (Holzman, Rivas, & Piccolo, 2014).

Band 2 data were selected to calculate the SMA. Nine scenes which were coincident with run-off events of significant magnitude were analysed. It should be noted that a possible limitation of the method to retrieve SMA at 250-m spatial resolution can be the mixed-pixel effect in small and heterogeneous basins. Considering this aspect, only events registered during autumn or winter were selected, because during these seasons, according to Varni, Entraigas, and Ares (2008), the watershed is predominantly under fallow or with winter crops in early stages of growth (Figure 1b). As a consequence, soil cover with actively growing vegetation is very low, poor hydrologic condition dominates, and evapotranspiration is low. Thus, the surface condition of the basin is uniform, and the signal is dominated by low-covered and bare soil at the analysed scale. The scenes included in the analyses corresponded to dates previous to rainfall events and subsequent to the corresponding peak flows registered in the gauging station and are indicated in Figure 2. Other scenes were processed to consider a wider temporal trend of surface moisture, which included the available data during the period between 12 days before the peak of the run-off events analysed and 6 days after the date of the run-off peak.

To detect surface moisture, an observational threshold criterion was applied analysing basic statistics of water and moist soil areas. The chosen surface reflectance threshold value varied between 0.15 and 0.18, considering that all values below it corresponded to free surface water or moist soil. This threshold was consistent with reflectance values for saturated soils showed in previous works (Fabre, Briottet, & Lesaignoux, 2015; Tian & Philpot, 2014). A mask containing the values of interest was built, and the percentage area of surface moisture previous to the events (prev-SMA, %) and subsequent to the events (post-SMA, %) were calculated. Because there was no cloud free scene previous to event number six, whose run-off started on July 13, 2014, no mask could be built for that case.

2.3 | Rainfall data

The rainfall was measured by six automatic weather stations located in the study area (Figure 1a). The rain gauges are constructed

according to the World Meteorological Organization, which record the rain every minute with an accuracy of 0.20 mm through a tipping bucket recording rain gauge. The rainfall over the watershed was calculated hourly using the Thiessen polygons method for each rainfall associated with a run-off event. This method computes a regional precipitation value as a weighted average of point measured values (Dingman, 2015).

The calculated rainfall variables were total precipitation depth (P , mm) and maximum intensity of rainfall over 6 hr ($I6_{max}$, mm h^{-1}), calculated as the maximum of the rainfall averages over 6 hr for each rainfall event associated with run-off.

2.4 | Run-off data

Stream water levels were registered at Seminario station, located at the outlet of the middle basin (Figure 1a). The levels were measured with a pressure sensor every hour. The records were turned into flow through the stage-discharge rating curve of the section, obtained by stream discharge measurements conducted with current meters. Total run-off separation in direct and base flow was performed by applying a digital filter (Rodríguez, Vionnet, Parkin, & Younger, 2000) based on one of the methods reviewed by Nathan and McMahon (1990) and Chapman (1999). The filter removes the high frequency component of the hydrograph (i.e., direct run-off) and determines the low frequency component (i.e., the base flow).

The run-off variables considered in this study were surface run-off registered between the beginning of the event and the day previous to the analysed MODIS scene (R , mm), total surface run-off calculated between the beginning and the end of the event (R_t , mm), peak flow (Q_p , $\text{m}^3 \text{s}^{-1}$). Flood intensity (IF , $\text{m}^3 \text{min}^{-1}$), which describes the discharge speed to reach the peak flow during a flood event (Oeurng, Sauvage, & Sánchez-Pérez, 2010), was calculated by Equation 1:

$$IF = \frac{(Q_p - Q_b)}{T_p}, \quad (1)$$

where Q_b is the baseflow at the beginning of the event ($\text{m}^3 \text{s}^{-1}$) and T_p is the time to peak (h).

Events over $20 \text{ m}^3 \text{s}^{-1}$, which were considered of a relevant magnitude according to the basin area and the climatic characteristics of the region, were included in this analysis. Depending on rainfall and run-off data, and MODIS scenes availability, nine run-off events were analysed. Figure 2 shows the cases studied in the context of the complete rainfall and run-off data for the years 2012, 2014, and 2015.

2.5 | Statistical analyses

Data normality was assessed using the Shapiro Wilk's test with a confidence interval level of 95% (Di Rienzo et al., 2015). The variables post-SMA, prev-SMA, P , $I6_{max}$, R , R_t , and Q_p were normally distributed ($p > .05$). The flood intensity data did not show normal distribution ($p < .05$) and a square root transformation was applied to these data. The new variable was identified as IF_r .

Considering the available data and following the parsimony principle, the simplest model was selected to describe and explain the relationships found (Montgomery, Peck, & Vining, 2002): The simple

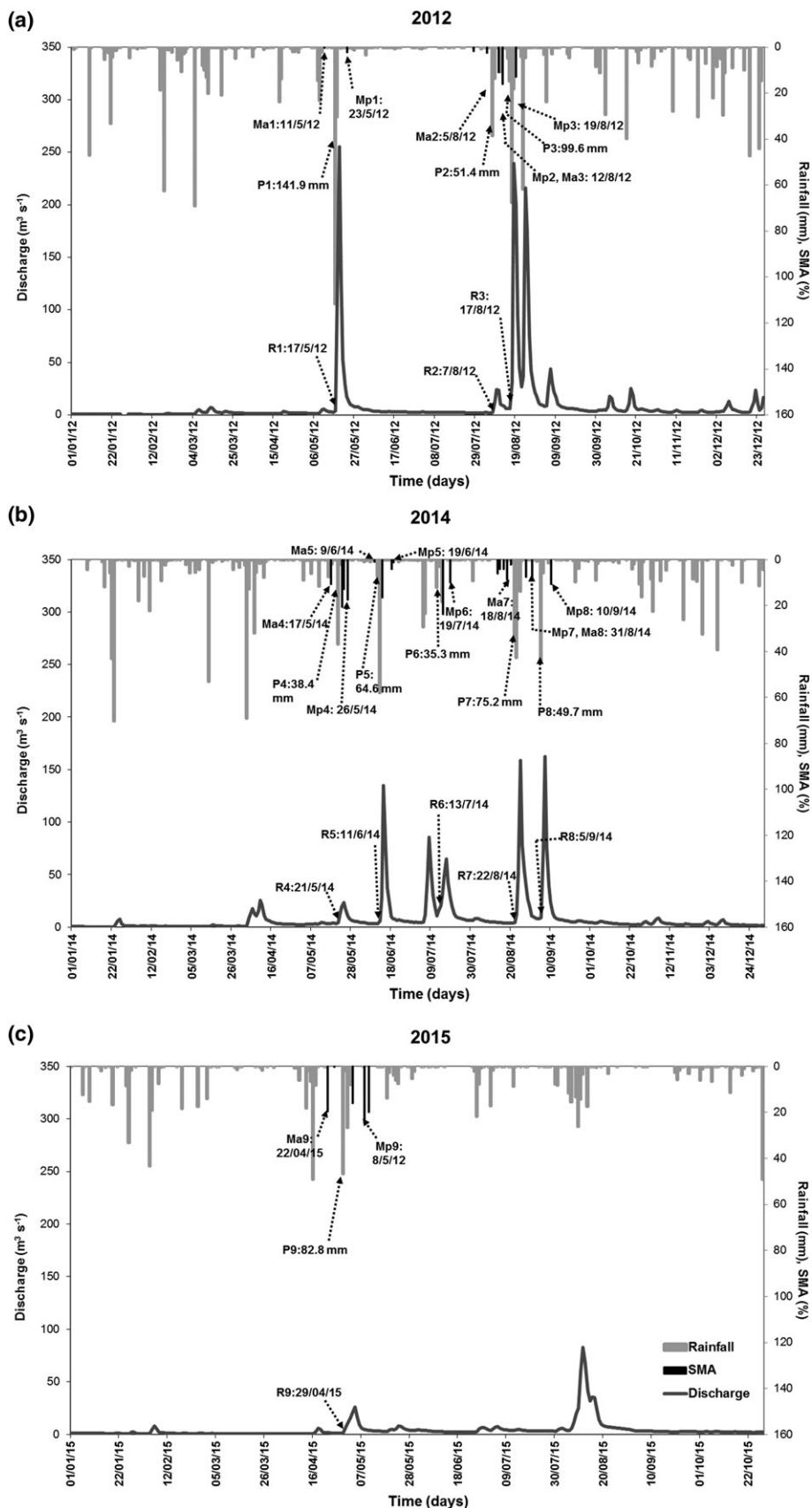


FIGURE 2 Daily rainfall and run-off data for the years 2012, 2014, and 2015. The studied cases are identified by the run-off start date (R), and by the date of the MODIS scenes which were analysed previous to the event (Ma), and subsequent to run-off peak (Mp), followed by the event number. The corresponding rainfall (P) of each event is also indicated. Soil moisture area (SMA) obtained from MODIS scenes includes the available data of the period between 12 days before the peak of the run-off events analysed and 6 days after the date of the run-off peak. Run-off data available for the year 2015 include the period 01/01–27/10

linear regression models between post-SMA and P, I_{6max} , R, Qp, and IFr were performed. In addition, the simple linear regressions between IFr and I_{6max} , Rt and I_{6max} , and R and prev-SMA were analysed, to explain different aspects of the relationships between post-SMA and the considered hydrological variables.

The linear regression significance between the variables was tested, and the models were assessed by the coefficient of determination (R^2). The models were tested for normality of the error terms using Shapiro Wilk's test with a confidence interval level of 95%. Independence of errors and homogeneity of variance of the errors' terms of the models were analysed with the plot of studentized residuals versus the fitted values (Myers, 1990).

3 | RESULTS

The main characteristics of the events studied are summarized in Table 1. Figure 2 also shows total precipitation of each analysed case and SMA values obtained. The events included a variety of conditions in relation with minimum and maximum values of rainfall, its intensity, and run-off response.

The SMA subsequent to the peak discharge (post-SMA) showed values above the mean (11.3%) in four of the nine examined situations. Figure 3 shows the SMA previous to the events (prev-SMA) and the post-SMA obtained for three scenes corresponding to the dates with maximum and minimum post-SMA and the case with the closest value to the calculated average post-SMA.

Most of the analysed cases corresponded to 2012 and 2014 autumns-winters, seasons with rainfalls of 91.1 and 106.1 mm, respectively, which are above the 30-year seasonal mean (56 mm). These particularly rainy seasons generated overflows of different magnitude which affected Azul city in three times during 2012 (18/05/2012; 17/08/2012; 23/08/2012).

Considering the linear regression models performed (Table 2), the identified post-SMA showed negative and statistically significant linear relationships with the run-off registered between the beginning of the event and the day previous to the MODIS scene analysed subsequent to peak discharge (R; $p < .05$). Surprisingly, SMA was smaller during events with high run-off than during those with low run-off and peak flows recorded at the outlet of the basin. The relationship between R and prev-SMA showed the same trend (Table 2).

TABLE 1 Mean, maximum and minimum values of the variables analysed for the nine studied events in the watershed of the Del Azul.

Variable	Minimum	Maximum	Mean
post-SMA (%)	1.4	23.1	11.3
prev-SMA (%)	0.43	19.6	10.3
P (mm)	35.3	141.9	70.9
I_{6max} (mm h ⁻¹)	2.8	10.7	5.7
R (mm)	3.2	36.7	15.3
Rt (mm)	3.5	36.9	9.8
Qp (m ³ s ⁻¹)	3.5	36.9	17.5
IFr (m ^{3/2} min ^{-1/2})	0.48	2.7	1.5

The model between post-SMA and peak flow (Qp) also showed negative trend with statistical significance ($p < .05$), but the residuals were not independent and did not show homogeneous variance. The linear relationship between post-SMA and IFr was not statistically significant ($p > .05$).

The post-SMA also showed a negative linear relationship with the maximum intensity of rainfall over 6 hr (I_{6max} ; $p < .05$), but post-SMA and precipitation did not show a statistically significant linear relationship. In addition, statistically significant relationships between IFr and I_{6max} and Rt and I_{6max} were found, with normally distributed and independent residuals, and of homogeneous variance. These relations suggest the relevance of I_{6max} in the speed of water transport within the basin and on run-off response (Nu-Fang, Zhi-Hua, Lu, & Cheng, 2011; Shi, Yan, Li, Li, & Cai, 2010).

4 | DISCUSSION

The negative linear relationships between post-SMA and R and between R and prev-SMA are notable. The maximum intensity of rainfall over 6 hr and its effect on run-off and its speed of transport along a basin with a particular geomorphology may be key factors involved in those negative relationships. The antecedent wetness may have also conditioned the response found by interacting with I_{6max} , as it is analysed below. The post-SMA did not show clear statistical relationships with the hydrological variables Qp and IFr. Only the variable IFr will be considered to discuss the mentioned negative trends, as it is highly correlated with Qp (Pearson correlation coefficient of 0.99, $p < .05$).

Some authors found positive relationships between water-saturated area and river stage in plain basins of Siberia (Papa et al., 2008) and the north and centre of South America (Hamilton, Sippel, & Melack, 2004) considering monthly data of several years. According to their hydrological dynamics, these watersheds are regularly subjected to seasonal inundation. In contrast, the watershed under study is characterized by the occurrence of floods not regularly predictable, where humid periods are followed by droughts or by others without flooding conditions, but not in a regular seasonal pattern (Kuppel, Houspanossian, Nosoetto, & Jobbágy, 2015; Scarpati & Capriolo, 2013). In relation with this particular tendency, our study was carried out at individual events scale, to understand which variables contribute to the hydrological response of the events evaluated in terms of the SMA. In our case, making a monthly analysis using data of several years would have masked important events which may cause overflows and that are of critical interest for the region. In addition, this watershed has a particular geomorphology, in which plain areas coexist with gentle slopes. This characteristic combined with the variables that influence run-off response and the underlying processes which generate run-off may explain the negative relationships between water-saturated area and river stage, as it is discussed below.

The interaction between the rate of input, the storage, and the hydrological response may guide the identification of the dominant processes which contribute to run-off generation (Spence, 2010). Hortonian overland flow takes place when rainfall rate surpasses

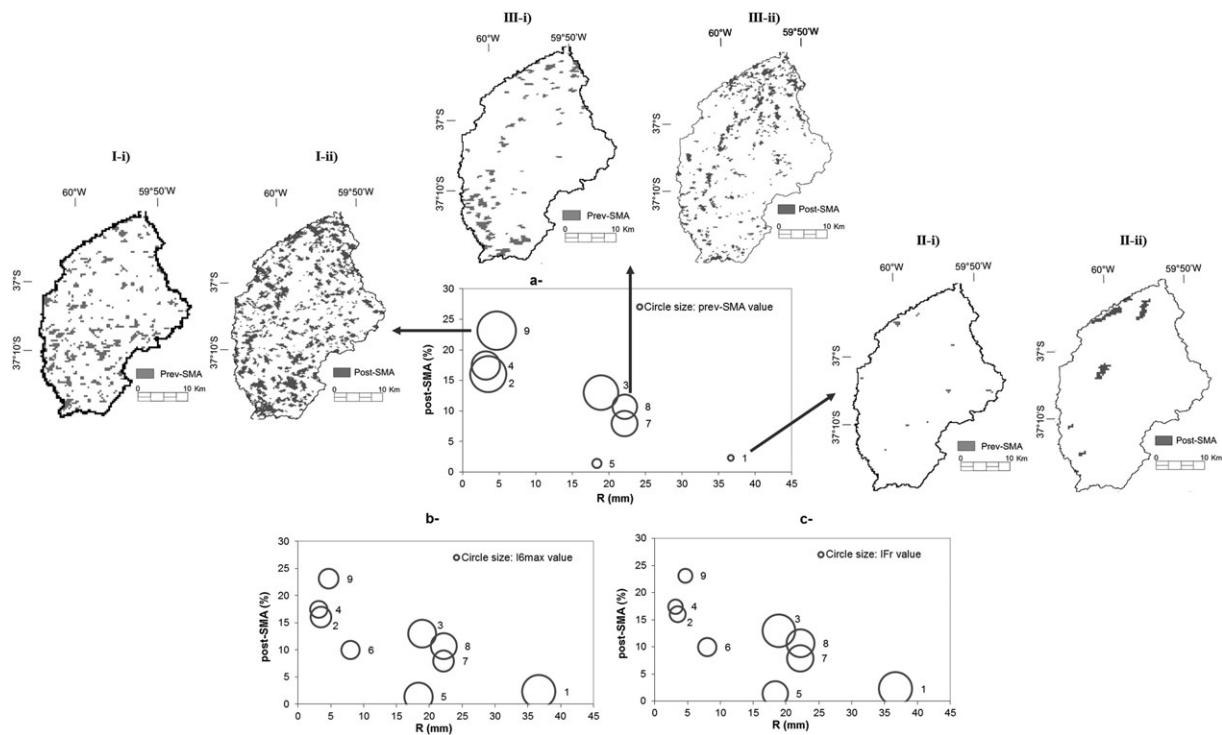


FIGURE 3 Relationship between the area of surface moisture subsequent to run-off peak discharge obtained from MODIS scenes (post-SMA, %), the associated surface run-off (R , mm) and (indicated by circle size): (a) the surface moisture previous to the beginning of each event (prev-SMA), (b) the maximum intensity of rainfall over 6 hr (16_{max}), (c) the square root of the flood intensity (IFr). Images of pre-SMA (i) and post-SMA (ii) are included: I) maximum area (i: 22/04/2015; ii: 08/05/2015), II) minimum area (i: 11/05/2012; ii: 23/05/2012), III) the case with the closest value to the calculated average area (i: 31/08/2014; ii: 10/09/2014)

TABLE 2 Linear regression models, included variables, model coefficients, performance, and assumptions including the adjusted regression coefficients. Each linear model was tested for normality, independence and variance homogeneity of residuals

Linear regression models						Model's assumptions	
Variable		Regression coefficients		Linear regression significance		Residuals' normality	Independence and variance homogeneity of residuals
Dependent	Independent	Slope of regression line	Intercept	p value	R^2	p value	
Post-SMA	P	-0.07	16.20	>.05	0.11	>.05	Not satisfied
Post-SMA	16_{max}	-1.81	21.57	<.05	0.46	>.05	Satisfied
Post-SMA	R	-0.48	18.62	<.05	0.59	>.05	Satisfied
Post-SMA	Q_p	-0.05	17.77	<.05	0.47	>.05	Not satisfied
Post-SMA	IFr	-5.08	18.75	>.05	0.41	>.05	Not satisfied
IFr	16_{max}	0.29	-0.18	<.05	0.74	>.05	Satisfied
R_t	16_{max}	4.19	-6.29	<.05	0.71	>.05	Satisfied
R	Prev-SMA	-1.20	28.54	<.05	0.54	>.05	Satisfied

the infiltration capacity of soils (Mishra & Singh, 2003). Saturated overland flow results from the saturation of the surface soil horizon as a consequence of the presence of a subsurface horizon of lower hydraulic conductivity or from the rise of a shallow water table (Pilgrim & Cordery, 1993). Dingman (2015) points out differences in run-off generation mechanisms according to peak run-off rates. Montgomery and Dietrich (1995) also report different run-off mechanisms under different wetness conditions. Dry previous conditions are, in general, related to Hortonian overland flow, whereas saturated overland flow is related to wet previous conditions (Lana-Renault, Regués, Serrano, & Latron, 2014; Saffarpour, Western, Adams, & McDonnell, 2016; Smith & Goodrich, 2005).

Smith and Goodrich (2005) express that both mechanisms may occur in the same watershed and even at a same point in a watershed. Meanwhile, Orchard, Lorentz, Jewitt, and Chaplot (2013) discuss that overland flow is a consequence of the interactions between different spatially variable factors (rainfall intensity, evapotranspiration, soil moisture patterns, land use, etc.). Thus, this leads to the coexistence of the run-off mechanisms at different sites of a basin during the same event and/or between different events (Saffarpour et al., 2016).

Considering the data set analysed and the relationships shown in Figure 3, three groups of cases defined by combined values of rate of *input* (analyzed by rainfall intensity), *antecedent condition* (analyzed

by the previous SMA), and *hydrologic response* (in terms of surface run-off) may be defined:

- a. events of low rainfall intensity, high antecedent moisture, and low run-off (events 2, 4, 6 and 9);
- b. events of high rainfall intensity, low antecedent moisture, and medium to high run-off (events 1 and 5);
- c. events of medium to high rainfall intensity, medium to high antecedent moisture, and medium run-off (events 3, 7 and 8).

During events of high antecedent moisture and low rainfall intensities, run-off at the outlet of the middle basin showed the lowest values with the lowest flood intensities that indicate that run-off flowed slowly down the basin. Then, water had a longer overland residence time in comparison with the other events. This increased the infiltration potential and water storage. In addition, shallow soils in the area had more chances to become saturated. According to the low peak discharges and low rainfall intensities, Dingman (2015) and Latron and Gallart (2008) related events of these characteristics to saturated overland flow. The plain areas and wetlands of the basin expressed their storage capacity in these cases: Paoli and Giacosa (1983) pointed out that in areas of low regional slopes, every little pond and depression act as reservoirs that diminish the volume of surface water to run-off. This favours the expression of retention and detention of plain areas and wetlands, in addition to weakly channelized water flow. The response during these events associated with the geomorphological characteristics contrasts with the high run-off reported by Latron and Gallart (2008) in a Mediterranean watershed with humid climate and mean slope of 25.8% under previous wet conditions. These authors also reported large saturated areas within the watershed, registered by visual observations. In our case, according to Orchard et al. (2013), the plain areas and wetlands at the headwaters combined with the events characteristics and the previous conditions may have been important in the generation of saturated overland flow. In addition, the increment of the humid area of riparian zones and temporal path flows, which was studied by Ares et al. (2016) in the approach of hydrological and sedimentological connectivity in the upper basin of the Del Azul stream, may evidence the occurrence of this mechanism. Thus, these situations evidence the particular water dynamics in the basin, supported by the highest surface moisture values obtained after peak discharge, above 10% of the area.

Events of low antecedent moisture and high rainfall intensity were associated with medium to high run-off magnitude and IFR. These events were rapidly transported along the gentle hillslopes in the upper and middle basins to the water course by the drainage network and water stayed during short times on land surface. In these cases, rainfall intensity commanded a quick and channelized water output from the basin, and water did not stay in the watershed to increase wetness; therefore, the area of surface moisture remained low.

Janzen and McDonnell (2015) and Saffarpour et al. (2016) also reported significant run-off under dry previous conditions with high rainfall intensities in watersheds of humid climate and slopes of

23.3% and between 2% and 50%, respectively. In this sense, Janzen and McDonnell (2015) pointed out that under low antecedent moisture, high accumulated rainfall or high rainfall intensities are the necessary conditions to generate high run-off. However, in the studies conducted by Latron and Gallart (2008), small run-off depths were registered under the same conditions, but they also found no saturated area in the catchment.

Events 1 and 5 may be associated with Hortonian overland flow, in relation to their high run-off peaks (Dingman, 2015), high rainfall, and flow intensities. Low vegetation cover and shallow soils may have favoured the generation of this mechanism. Bare or almost bare land surface occupies a relevant surface during autumn and winter in the study area (Varni et al., 2008), the seasons under analysis. Thus, vegetation cover, which prevents soils from sealing by raindrop impact, is reduced. Seals and crusts decrease infiltration and enhance Hortonian overland flow (Kirkby, 2005). In studies conducted in the upper basin of the Del Azul stream, Ares, Chagas, and Varni (2014) pointed out the relevance of land cover to control run-off: The authors obtained average final infiltration rates of 34.3 mm h⁻¹ for bare soils and 115.5 mm h⁻¹ for soils under no tillage covered by wheat stubble in 100%, during rainfall simulations. Dry antecedent conditions may favour the sealing process as dry soil aggregates show higher aggregate detachability than humid aggregates (Vermang, Demeyer, Cornelis, & Gabriels, 2009), which was corroborated for the Del Azul basin soils. In the same area previously mentioned, Ares et al. (2016) registered important erosion signs (seals and rills) as a consequence of event 1 which was related to high discharge and IFR. Hueso-González, Ruiz-Sinoga, Martínez-Murillo, and Lavee (2015) reported the occurrence of Horton's flow in dry bare soils of Spain, under high rainfall intensities which originated quick and sharp run-off responses.

The third group of events is associated with more heterogeneous *input-antecedent conditions* than the cases in groups 1 and 2 and response results in medium run-off with medium saturated area and high flood intensity.

The dominating run-off mechanism within a watershed is the result of the combination of land slope, soil vegetation cover, soil type and thickness, and local distribution of meteorological factors (Spence, 2010). The heterogeneity of landscape topography is indeed recognized as a key factor contributing to differences in run-off generation mechanism (Allan & Roulet, 1994). In addition, Spence (2010) pointed out that the interaction between the spatial distribution of landscape units and topography controls the storage of the basin and the necessary connections to run-off generation. Thus, the available data up to now may indicate that the conditions registered during these events may have led to a spatially variable run-off response related to the interactions between the particular geomorphological characteristics of the basin, the previous surface moisture conditions, and the differences in rainfall intensities. Therefore, it is probable that some areas produced Hortonian overland flow and some others saturated overland flow, under local spatial conditions comparable to those described for groups 1 and 2, respectively. Then, some areas may have generated large discharges, and others low discharges. This spatial variability of factors, which determines the coexistence of different run-off mechanisms, has

been reported by Lana-Renault et al. (2014), who pointed out that consequently the local hydrological responses are complex under these conditions. As a result, the final run-off response at the outlet of the catchment, of medium magnitude in comparison with the other events analysed, may be an average of those spatially variable responses and is associated with medium SMA after peak discharges.

The performed analyses suggest that run-off response and the associated moisture area in the study area are dependent not only on antecedent moisture or maximum rainfall intensity but also on the interactions between these factors with the geomorphology of the landscape. These interactions may determine the predominance or the combination of Hortonian overland flow and/or saturated overland flow. In coincidence with Saffarpour et al. (2016), it is also important to highlight the existence of run-off processes induced not only by previous wetness but also by rainfall intensity, not frequently reported in previous works for humid areas under agriculture. In this sense, our results contribute to the understanding of the coexistence of different run-off mechanisms and may be also important from the perspective of the modelling of these processes together, a topic of current interest in hydrology (Li & Sivapalan, 2014; Wang, Chen, Bao, & Zhang, 2017).

5 | SUMMARY AND CONCLUSIONS

This manuscript studies the relationships between SMA extracted from satellite images analysis and a set of hydrological variables corresponding to individual rainfall-run-off events registered in a plain basin of the Argentine Pampas Region. In contrast with previous studies, which were carried out at a monthly scale, the relationship between the surface moisture retrieved from daily MODIS surface reflectance data and the run-off of the events associated with the scenes subsequent to peak discharges showed a statistically significant negative linear relationship. Likewise, the relationship between the surface moisture and maximum rainfall intensity over 6 hr showed the same trend. In addition, the square root of the run-off intensity and I_{\max} was positively related, which indicates that rainfall intensity is associated with the speed of water output from the basin.

The joint analyses between *rate of input-antecedent condition-hydrological response* contributed to identify the predominant run-off mechanisms during the events. These mechanisms, in relation to the particular geomorphological characteristics of the basin, helped to explain the negative relationships between post-SMA and R. Events of low rainfall intensity, high antecedent moisture, and low run-off were possibly associated with saturated overland flow. In these cases, water transport was slow: The buffering effect of plain areas and depressions became important and flow run weakly channelized, water stayed longer on the land surface, and added to the water already stored in the watershed. As a result, a large SMA remained after peak discharge.

During events of high rainfall intensity, low antecedent moisture and medium to high run-off Hortonian overland flow may have prevailed. In these cases, rainfall intensity induced a quick and

channelized transport of run-off down the hillslopes, high I_{Fr}, and surface water permanence for short periods. This response was associated with that of sloped watersheds, and the conditions described may have determined the small SMA.

Events of medium to high rainfall intensity, medium to high antecedent moisture, and medium run-off were related to more heterogeneous input-antecedent-run-off responses than the previous cases. Thus, it is possible that local spatial conditions may have produced Hortonian overland flow or saturated overland flow leading to an averaged response as a result of the local variability along the watershed. Therefore, medium SMA was detected.

This work shows the first analysis of these relationships for the region. Considering the method used to obtain SMA, it should be noted that although the surface reflectance of soil moist and flooded area is a physical property, threshold to define SMA can vary according to soil types, slopes. That threshold should be checked in the area where the method will be implemented.

According to our results, it is important to mention that the incorporation of future data may evidence possible non-linear trends. However, this first interpretation of the relationships is considered essential to improve the understanding of the complex hydrological dynamics of basins where gently slopes coexist with neighbouring plain lands. These hydrological systems show highly variable responses corresponding to floods not regularly predictable. Thus, the examples reported in our work may be particularly interesting in the context of climate change. Besides, the analyses carried out are key to the development of the hydrological modelling of plain watersheds, which needs a comprehensive vision of these systems to explain their particular dynamics. Finally, our work is relevant for the general knowledge of the hydrology of large plain areas around the world, whose functioning studies are still in their early stages.

ORCID

María Guadalupe Ares  <http://orcid.org/0000-0002-6992-6974>

REFERENCES

- Ahmad, A., Zhang, Y., & Nichols, S. (2011). Review and evaluation of remote sensing methods for soil-moisture estimation. *SPIE Reviews*, 2, 028001-1-028001-17. <https://doi.org/10.1117/1.3534910>
- Allan, C. J., & Roulet, N. T. (1994). Runoff generation in zero-order precambrian shield catchments: The stormflow response of a heterogeneous landscape. *Hydrological Processes*, 8, 369-388.
- Amani, M., Parsian, S., Mirmazloumi, S. M., & Aieneh, O. (2016). Two new soil moisture indices based on the NIR-red triangle space of Landsat-8 data. *International Journal of Applied Earth Observation and Geoinformation*, 50, 176-186.
- Aragón, R., Jobbágy, E. G., & Viglizzo, E. F. (2010). Surface and groundwater dynamics in the sedimentary plains of the Western Pampas (Argentina). *Ecohydrology*, 4, 433-447. <https://doi.org/10.1002/eco.149>
- Ares, M. G., Bongiorno, F., Holzman, M., Chagas, C., Varni, M., & Entraigas, I. (2016). Water erosion and connectivity analysis during a year with high precipitations in a watershed of Argentina. *Hydrology Research*, 47, 1239-1252. <https://doi.org/10.2166/nh.2016.179>
- Ares, M. G., Chagas, C., & Varni, M. (2014). Respuesta hidrológica de cuencas de diferentes tamaños ubicadas en la Pampa Serrana y en la Pampa Ondulada. *Ciencia del Suelo*, 32, 117-127.

- Baker, C., Lawrence, R. L., Montagne, C., & Patten, D. (2007). Change detection of wetland ecosystems using Landsat imagery and change vector analysis. *Wetlands*, 27, 610–619.
- Brakenridge, R., & Anderson, E. (2006). MODIS-based flood detection mapping and measurement: The potential for operational hydrological applications. In J. Marsalek, G. Stancalie, & G. Balint (Eds.), *Transboundary floods: Reducing risks through flood management* (pp. 1–12). Dordrecht: Springer.
- Canosa, F. R., Feldkamp, C., Urruti, J., Morris, M., & Moscoso, M. R. (2013). *Potencial de la producción ganadera ante diferentes escenarios*. Report of Producir Conservando Foundation: Argentina. 82 pp
- Chapman, T. (1999). A comparison of algorithms for stream flow recession and baseflow separation. *Hydrological Processes*, 13, 701–714.
- Chen, Y., Huang, C., Ticehurst, C., Merrin, L., & Thew, P. (2013). An evaluation of MODIS daily and 8-day composite products for floodplain and wetland inundation mapping. *Wetlands*, 33, 823–835. <https://doi.org/10.1007/s13157-013-0439-4>.
- Dalponete, D., Rinaldi, P., Cazenave, G., Usunoff, E., Varni, M., Vives, L., ... Clause, A. (2007). A validated fast algorithm for simulation of flooding events in plains. *Hydrological Processes*, 21, 1115–1124. <https://doi.org/10.1002/hyp.6301>
- Di Rienzo, J. A., Casanoves, F., Balzarini, M. G., Gonzalez, L., Tablada, M., & Robledo, C. W. (2015). *InfoStat versión 2015*. Grupo InfoStat: FCA, Universidad Nacional de Córdoba, Argentina.
- Dingman, S. L. (2015). *Physical hydrology*. (p. 643) Waveland press.
- Dunne, T., Moore, T. R., & Taylor, C. H. (1975). Recognition and prediction of runoff producing zones in humid regions. *Hydrological Sciences Bulletin*, 20, 305–327.
- Fabre, S., Briottet, X., & Lesaignoux, A. (2015). Estimation of soil moisture content of bare soils from their spectral optical properties in the 0.4–12 μm spectral domain. *Sensors*, 15, 3262–3281. <https://doi.org/10.1109/ISARSS.2010.5649907>.
- Frazier, P., Page, K., Louis, J., Briggs, S., & Robertson, A. I. (2003). Relating wetland inundation to river flow using Landsat TM data. *International Journal of Remote Sensing*, 24, 3755–3770. <https://doi.org/10.1080/0143116021000023916>
- Gao, Z., Xu, X., Wang, J., Yang, H., Huang, W., & Feng, H. (2013). A method of estimating soil moisture based on the linear decomposition of mixture pixels. *Mathematical and Computer Modelling*, 58, 606–613.
- Ghulam, A., Qin, Q., Teyip, T., & Li, Z. L. (2007). Modified perpendicular drought index (MPDI): A real-time drought monitoring method. *ISPRS Journal of Photogrammetry and Remote Sensing*, 62, 150–164. <https://doi.org/10.1016/j.isprsjprs.2007.03.002>
- Hamilton, S. K., Sippel, S. J., & Melack, J. M. (2002). Comparison of inundation patterns among major South American floodplains. *Journal of Geophysical Research*, 107(D20). <https://doi.org/10.1029/2000JD000306>
- Hamilton, S. K., Sippel, S. J., & Melack, J. M. (2004). Seasonal inundation patterns in two large savannah floodplains of South America: The Llanos de Moxos (Bolivia) and the Llanos del Orinoco (Venezuela and Colombia). *Hydrological Processes*, 18, 2103–2116. <https://doi.org/10.1002/hyp.5559>
- Hansen, M. C., Townshend, J. R. G., DeFries, R. S., & Carroll, M. (2005). Estimation of tree cover using MODIS data at global, continental and regional/local scales. *International Journal of Remote Sensing*, 26, 4359–4380. <https://doi.org/10.1080/01431160500113435>
- Holzman, M. E., & Rivas, R. (2016). Early maize yield forecasting from remotely sensed temperature/vegetation index measurements. *IEEE Journal of Selected Topics in Applied Earth Observations and Remote Sensing*, 9, 507–519. <https://doi.org/10.1109/JSTARS.2015.2504262>
- Holzman, M. E., Rivas, R., & Bayala, M. (2014). Subsurface soil moisture estimation by VI–LST method. *IEEE Geoscience and Remote Sensing Letters*, 11, 1951–1955. <https://doi.org/10.1109/LGRS.2014.2314617>
- Holzman, M. E., Rivas, R., & Piccolo, M. C. (2014). Estimating soil moisture and the relationship with crop yield using surface temperature and vegetation index. *International Journal of Applied Earth Observation and Geoinformation*, 28, 181–192.
- Huang, C., Chen, Y., & Wu, J. (2014). Mapping spatio-temporal flood inundation dynamics at large river basin scale using time-series flow data and MODIS imagery. *International Journal of Applied Earth Observation and Geoinformation*, 26, 350–362.
- Hueso-González, P., Ruiz-Sinoga, J. D., Martínez-Murillo, J. F., & Lavee, H. (2015). Overland flow generation mechanisms affected by topsoil treatment: Application to soil conservation. *Geomorphology*, 228, 796–804.
- INTA (Instituto Nacional de Tecnología Agropecuaria) (1989). *Mapa de Suelos de la Provincia de Buenos Aires*. Buenos Aires, Argentina: Escala 1:500.000. Secretaría de Agricultura, Ganadería y Pesca; Instituto de Evaluación de Tierras (CIRN-INTA).
- INTA (Instituto Nacional de Tecnología Agropecuaria) (1992). *Carta de Suelos de la República Argentina*. Buenos Aires, Argentina: Hojas 3760-16 (16 de julio), 3760-21 (Azul) 3760-22 (Chillar), 1:50,000. INTA.
- Janzen, D., & McDonnell, J. J. (2015). A stochastic approach to modelling and understanding hillslope runoff connectivity dynamics. *Ecological Modelling*, 298, 64–74.
- Jensen, J. R. (2007). *Remote sensing of the environment: An earth resource perspective* (2nd ed.). Upper Saddle River, NJ: Prentice Hall.
- Jobbágy, E. G., Noretto, M. D., Santoni, C. S., & Baldi, G. (2008). El desafío ecohidrológico de las transiciones entre sistemas leñosos y herbáceos en la llanura Chaco-Pampeana. *Ecología Austral*, 18, 305–322.
- Khan, S. I., Hong, Y., Wang, J., Yilmaz, K. K., Gourley, J. J., Adler, R. F., ... Irwin, D. (2011). Satellite remote sensing and hydrologic modeling for flood inundation mapping in Lake Victoria basin: Implications for hydrologic prediction in ungauged basins. *IEEE Transactions on Geoscience and Remote Sensing*, 49, 85–95.
- Kirkby, M. J. (2005). Organisation and process. In M. G. Anderson (Ed.), *Encyclopedia of hydrological sciences*, vol. 1 (pp. 41–58). Chichester, UK: John Wiley.
- Klein, I., Dietz, A. J., Gessner, U., Galayeva, A., Myrzhakmetov, A., & Kuenzer, C. (2014). Evaluation of seasonal water body extents in Central Asia over the past 27 years derived from medium-resolution remote sensing data. *International Journal of Applied Earth Observation and Geoinformation*, 26, 335–349.
- Kovács, G. (1983). General principles of flat-land hydrology. In M. C. Fuschini Mejía (Ed.), *Hidrología de las grandes llanuras* (pp. 297–357). Buenos Aires, Argentina: UNESCO-Secretaría Nacional de Recursos Hídricos.
- Kruse, E., & Zimmermann, E. (2002). Hidrogeología de grandes llanuras: particularidades en la llanura pampeana (Argentina). In E. Bocanegra, D. Martínez, & H. Massone (Eds.), *Actas del Congreso Agua Subterránea y Desarrollo Humano* (pp. 2025–2038). Argentina: La Plata.
- Kuppel, S. S., Houspanossian, J., Noretto, M. D., & Jobbágy, E. G. (2015). What does it take to flood the Pampas?: Lessons from a decade of strong hydrological fluctuations. *Water Resources Research*, 51, 2937–2950. <https://doi.org/10.1002/2015WR016966>
- Lana-Renault, N., Regüés, D., Serrano, P., & Latron, J. (2014). Spatial and temporal variability of groundwater dynamics in a sub-Mediterranean mountain catchment. *Hydrological Processes*, 28, 3288–3299. <https://doi.org/10.1002/hyp.9892>
- Latron, J., & Gallart, F. (2008). Runoff generation processes in a small Mediterranean research catchment (Vallcebre, Eastern Pyrenees). *Journal of Hydrology*, 358, 206–220.
- Li, F., Crow, W. T., & Kustas, W. P. (2010). Towards the estimation root-zone soil moisture via the simultaneous assimilation of thermal and microwave soil moisture retrievals. *Advances in Water Resources*, 33, 201–214.
- Li, H.-Y., & Sivapalan, M. (2014). Functional approach to exploring climatic and landscape controls on runoff generation: 2 Timing of runoff storm response. *Water Resources Research*, 50, 9323–9342. <https://doi.org/10.1002/2014WR016308>

- Lobell, D. B., & Asner, G. P. (2002). Moisture effects on soil reflectance. *Soil Science Society of America Journal*, 66, 722–727.
- Magrin, G., Travasso, M. I., & Rodríguez, G. R. (2005). Changes in climate and crop production during the 20th century in Argentina. *Climate Change*, 72, 229–249. <https://doi.org/10.1007/s10584-005-5374-9>
- Mateucci, S. (2012). Ecorregión Pampa. In J. Morello, S. Mateucci, A. F. Rodríguez, & M. A. Silva (Eds.), *Ecorregiones y complejos ecosistémicos argentinos* (pp. 391–445). Buenos Aires, Argentina: Orientación Gráfica Editora.
- Mc Donnell, J. J. (2013). Are all runoff processes the same? *Hydrological Processes*, 27, 4103–4111. <https://doi.org/10.1002/hyp.10076>
- Milfred, C. J., & Kiefer, R. W. (1976). Analysis of soil variability with repetitive aerial photography. *Soil Science Society of America Journal*, 40, 553–557.
- Mishra, S. K., & Singh, V. (2003). *Soil conservation service curve number (SCS-CN) methodology*. Dordrecht, The Netherlands: Kluwer Academic Publishers.
- Montgomery, D. C., Peck, E. A., & Vining, G. G. (2002). *Introducción al análisis de regresión lineal*. (p. 588). Compañía Editorial Continental: México.
- Montgomery, D. R., & Dietrich, W. E. (1995). Hydrologic processes in a low-gradient source area. *Water Resources Research*, 31(1), 1–10. <https://doi.org/10.1029/94WR02270>
- Myers, R. H. (1990). *Classical and modern regression with applications* (2nd ed.). (p. 488). PWS-KENT: Boston, Massachusetts, USA.
- Nathan, R. J., & McMahon, T. A. (1990). Evaluation of automated techniques for baseflow and recession analysis. *Water Resources Research*, 26, 1465–1473.
- Njoku, E. G., & Entekhabi, D. (1996). Passive microwave remote sensing of soil moisture. *Journal of Hydrology*, 184, 101–129.
- Nu-Fang, F., Zhi-Hua, S., Lu, L., & Cheng, J. (2011). Rainfall, runoff, and suspended sediment delivery relationships in a small agricultural watershed of the Three Gorges area, China. *Geomorphology*, 135, 158–166.
- Oeurng, C., Sauvage, S., & Sánchez-Pérez, J. M. (2010). Dynamics of suspended sediment transport and yield in a large agricultural catchment, Southwest France. *Earth Surface Processes and Landforms*, 35, 1289–1301.
- Orchard, C. M., Lorentz, S. A., Jewitt, G. P. W., & Chaplot, V. A. M. (2013). Spatial and temporal variations of overland flow during rainfall events and in relation to catchment conditions. *Hydrological Processes*, 27, 2325–2338. <https://doi.org/10.1002/hyp.9217>
- Paoli, C., & Giacosa, R. (1983). Necesidades de investigaciones hidrológicas en áreas de llanuras. In M. C. Fuschini Mejía (Ed.), *Hidrología de las grandes llanuras* (pp. 395–430). Buenos Aires, Argentina: UNESCO-Secretaría Nacional de Recursos Hídricos.
- Papa, F., Prigent, C., & Rossow, W. B. (2008). Monitoring flood and discharge variations in the large Siberian rivers from a multi-satellite technique. *Surveys in Geophysics*, 29, 297–317. <https://doi.org/10.1007/s10712-008-9036-0>
- Petropoulos, G. P., Ireland, G., & Barrett, B. (2015). Surface soil moisture retrievals from remote sensing: Current status, products & future trends. *Physics and Chemistry of the Earth, Parts A/B/C*, 83–84, 36–56.
- Pilgrim, D. H., & Cordery, I. (1993). In D. R. Maidment (Ed.), *Flood runoff*. In *Handbook of hydrology* (pp. 9.1–9.42). New York, U.S.A: McGraw-Hill Inc.
- Quiroz Londoño, O. M., Romanelli, A., Lima, M. L., Massone, H. E., & Martínez, D. E. (2016). Fuzzy logic-based assessment for mapping potential infiltration areas in low-gradient watersheds. *Journal of Environmental Management*, 176, 101–111.
- Rodríguez, L. B., Vionnet, C., Parkin, G., & Younger, P. (2000). *Aplicación de un método automático para la separación de las componentes del hidrograma*. (pp. 279–286). Argentina: Actas del XIX Congreso Latinoamericano de Hidráulica Córdoba.
- Rodríguez-Blanco, M. L., Taboada-Castro, M. M., & Taboada-Castro, M. T. (2012). Rainfall-runoff response and event-based runoff coefficients in a humid area (Northwest Spain). *Hydrological Sciences Journal*, 57, 445–459. <https://doi.org/10.1080/02626667.2012.666351>
- Rokni, K., Ahmad, A., Selamat, A., & Hazini, S. (2014). Water feature extraction and change detection using multitemporal Landsat imagery. *Remote Sensing*, 6, 4173–4189. <https://doi.org/10.3390/rs6054173>
- Saffarpour, S., Western, A. W., Adams, R., & McDonnell, J. J. (2016). Multiple runoff processes and multiple thresholds control agricultural runoff generation. *Hydrology and Earth System Sciences*, 20, 4525–4545. <https://doi.org/10.5194/hess-20-4525-2016>
- Sala, J. M., Kruse, E., & Aguglino, R. (1987). *Investigación hidrológica de la Cuenca del Arroyo del Azul, Provincia de Buenos Aires*. Buenos Aires, Argentina: Informe 37.CIC.
- Scarpato, O. E., & Capriolo, A. D. (2013). Sequías e inundaciones en la provincia de Buenos Aires (Argentina) y su distribución espacio-temporal. *Investigaciones Geográficas*, (82), 38–51.
- Scioli, C. (2016). Un nuevo índice de similitud hidrológica para la simulación precipitación-escurrentía en sistemas de llanura. Doctoral thesis, Universidad Nacional del Litoral. Argentina; 106.
- Shi, Z. H., Yan, F. L., Li, L., Li, Z. X., & Cai, C. F. (2010). Interrill erosion from disturbed and undisturbed samples in relation to topsoil aggregate stability in red soils from subtropical China. *Catena*, 81, 240–248.
- Smith, R. E., & Goodrich, D. C. (2005). Rainfall Excess Overland Flow. In D. M. Anderson, & J. J. McDonnell (Eds.), *Encyclopedia of hydrological sciences* (pp. 1707–1718). Chichester, UK: John Wiley & Sons Ltd.
- Spence, C. (2010). A paradigm shift in hydrology: Storage thresholds across scales influence catchment runoff generation. *Geography Compass*, 4, 819–833. <https://doi.org/10.1111/j.1749-8198.2010.00341>
- Sriwongsitanon, N., Gao, H., Savenije, H. H. G., Maekn, E., Saengsawan, S., & Thianpopirug, S. (2015). The normalized difference infrared index (NDII) as a proxy for soil moisture storage in hydrological modelling. *Hydrology and Earth System Sciences Discussions*, 12, 8419–8457. <https://doi.org/10.5194/hessd-12-8419-2015>
- Tian, J., & Philpot, W. D. (2014). Spectral reflectance of drying soil. In *Geoscience and Remote Sensing Symposium, 2014 IEEE International*, IEEE, 3259–3262.
- Varni, M., Entraigas, I., & Ares, M. G. (2008). Evolución espacio-temporal del uso de la tierra a partir del procesamiento de imágenes Sac-C en la cuenca del arroyo del Azul (Argentina). *Revista de la ASAGAI -Geología Aplicada a la Ingeniería y al Ambiente*, 22, 99–105.
- Varni, M., Entraigas, I., Migueltorena, V., & Comas, R. (2013). Evaluation of flooded areas with satellite imagery using an objective hydrologic criterion. *Water and Environment Journal*, 27, 396–401. <https://doi.org/10.1111/j.1747-6593.2012.00356.x>
- Varni, M., Usunoff, E., Weinzettel, P., & Rivas, R. (1999). Groundwater recharge in the Azul aquifer, Central Buenos Aires Province, Argentina. *Physics and Chemistry of the Earth*, 24, 349–352.
- Vermang, J., Demeyer, V., Cornelis, W. M., & Gabriels, D. (2009). Aggregate stability and erosion response to antecedent water content of a loess soil. *Soil Science Society of America Journal*, 73, 718–726.
- Viglizzo, E. F., Jobbagy, E. G., Carreño, L., Frank, F. C., Aragón, R., De Oro, L., & Salvador, V. (2009). The dynamics of cultivation and floods in arable lands of Central Argentina. *Hydrology and Earth System Sciences*, 13, 491–502.
- Wang, L., Chen, D., Bao, H., & Zhang, K. (2017). On simulation improvement of the Noah_LSM by coupling with a hydrological model using a double-excess runoff production scheme in the GRAPES_Meso model. *Meteorological Applications*, 24, 512–520.
- Weidong, L., Baret, F., Gu, X. F., Tong, Q., Zheng, L., & Zhang, B. (2002). Relating soil surface moisture to reflectance. *Remote Sensing of Environment*, 81, 238–246.
- Wu, G., & Liu, Y. (2015). Downscaling surface water inundation from coarse data to fine-scale resolution: Methodology and accuracy assessment. *Remote Sensing*, 7, 15989–16003. <https://doi.org/10.3390/rs71215813>

- Zárate, M., & Mehl, A. (2010). Geología y geomorfología de la Cuenca del arroyo del Azul, provincia de Buenos Aires, Argentina. In M. Varni, I. Entraigas, & L. Vives (Eds.), *Hacia la gestión integral de los recursos hídricos en zona de llanuras* (pp. 65–78). Mar del Plata, Argentina: Editorial Martín.
- Zhu, Y., Weindorf, D. C., Chakraborty, S., Haggard, B., Johnson, S., & Bakr, N. (2010). Characterizing surface soil water with field portable diffuse reflectance spectroscopy. *Journal of Hydrology*, 391, 133–140.

How to cite this article: Ares MG, Holzman M, Entraigas I, Varni M, Fajardo L, Vercelli N. Surface moisture area during rainfall-run-off events to understand the hydrological dynamics of a basin in a plain region. *Hydrological Processes*. 2018;32:1351–1362. <https://doi.org/10.1002/hyp.11492>